

## Thermoreversible polymer gel electrolytes

A. M. Voice, J. P. Southall, V. Rogers, K. H. Matthews, G. R. Davies, J. E. McIntyre\* and I. M. Ward

IRC in Polymer Science and Technology and Department of Textile Industries, Leeds University, Leeds LS2 9JT, UK

(Received 26 August 1993; revised 17 January 1994)

Thermoreversible polymer gel electrolytes with ionic conductivities in the region of  $10^{-3} \text{ S cm}^{-1}$  (even at  $-20^\circ\text{C}$ ) have been prepared from a variety of commercially available polymers and organic solvents by gel casting from high-temperature solutions at polymer/solvent ratios down to 10/90. Lithium trifluoromethanesulfonate has been incorporated as the ionic species necessary for conduction. A typical gel has polymer/solvent in mass ratio 40/60 and has salt incorporated to give an active O/Li ratio of 12/1. In general, the dynamic modulus ( $G'$ ) of these gels is in excess of  $10^5 \text{ Pa}$  at low strain, but decreases rapidly with increasing strain amplitude despite remaining approximately constant with strain rate. This drop in modulus, which is attributed to breakdown of the gel network, is completely recoverable. In particular, one polymer, poly(vinylidene fluoride), was studied in detail. Gels made from this polymer formed self-supporting transparent films. The incorporation of lithium trifluoromethanesulfonate changed the crystal structure and decreased the solvent evaporation rate, at elevated temperatures, of poly(vinylidene fluoride) gels made with tetraethylene glycol dimethyl ether. Ionic conductivities of liquid electrolytes (dimethylformamide with lithium trifluoromethanesulfonate) and corresponding gels (dimethylformamide, lithium trifluoromethanesulfonate and poly(vinylidene fluoride)) suggest that there is no interaction between salt and polymer in these gels, although this is still under investigation.

(Keywords: polymer gel electrolyte; poly(vinylidene fluoride); lithium triflate)

### INTRODUCTION

Much of the research activity on polymer electrolytes has centred on systems related to poly(ethylene oxide) (PEO) following the initial discovery of Wright<sup>1</sup> that PEO formed crystalline complexes with alkali-metal salts. The practical application of PEO for batteries has been pioneered by Armand and his collaborators<sup>2</sup>. Other applications of solid electrolytes include sensors and display materials.

It is now appreciated that it is desirable to reduce or eliminate the crystallinity in these systems, for example by the development of amorphous comb polymers with PEO as the 'teeth' on a flexible polymeric backbone<sup>3</sup>. The ionic conductivity in solid polymer electrolytes can also be significantly increased by the addition of plasticizers<sup>4,5</sup>, essentially because these increase the molecular mobility of the polymer. The effectiveness of plasticizers in increasing the ionic conductivity has led to PEO systems with room-temperature conductivities in the region of  $10^{-3} \text{ S cm}^{-1}$ , but at the expense of mechanical rigidity, which appears to set a limit to the feasible achievement.

More recently, work has been carried out on polymer gel electrolytes based on plasticized polymers. These materials include a polymer, an ionic salt and a low-molecular-weight organic solvent. Tsuchida *et al.* report poly(vinylidene fluoride) (PVDF) gel electrolytes<sup>6-9</sup> with ionic conductivities in the region of  $10^{-5} \text{ S cm}^{-1}$  at or

around room temperature. A typical composition for their electrolytes is PVDF/propylene carbonate/lithium perchlorate in molar ratio 50/30/20. The same authors also report poly(acrylonitrile) (PAN) gel electrolytes<sup>9,10</sup> of typical composition PAN/ethylene carbonate/lithium perchlorate in molar ratio 50.7/36.6/12.7 having an ionic conductivity of  $2 \times 10^{-4} \text{ S cm}^{-1}$  at  $25^\circ\text{C}$ . Kabata *et al.*<sup>11</sup> have made crosslinked polymer gel electrolytes with an ambient conductivity of  $2.7 \times 10^{-3} \text{ S cm}^{-1}$  for a material consisting of 13 wt% monomer, 67 wt% solvent and 20 wt%  $\text{LiBF}_4$ , where the monomer is a mixture of ethoxypolyoxyethylene acrylate and trimethylolpropane triacrylate and the solvent is a mixture of propylene carbonate and 1,2-dimethoxyethane. Reich and Michaeli<sup>12</sup> report electrolytes consisting of PAN and hydrated perchlorate salts with ambient ionic conductivities in the range  $10^{-7}$  to  $10^{-2} \text{ S cm}^{-1}$ . In these systems the water acts as a plasticizer.

In this paper we report thermoreversible polymer gel electrolytes that have room-temperature conductivities in the region of  $10^{-3} \text{ S cm}^{-1}$ , combined with shear moduli in the region of  $10^5 \text{ Pa}$ . These gel electrolytes have a polymer/solvent mass ratio less than 1/1 and are the subject of a patent application<sup>13</sup>.

Many definitions of 'gel' exist. We have adopted the definition given by Almdal *et al.*<sup>14</sup>. Their two criteria for a gel are: (a) that the material consists of two or more components, one of which is a liquid, present in substantial quantity; and (b) that the material is soft and solid or solid-like with a storage modulus  $G'$  that exhibits a pronounced plateau extending to times of the order of

\* To whom correspondence should be addressed

seconds, and a loss modulus  $G''$  that is considerably smaller than  $G'$  in the plateau region.

## EXPERIMENTAL

### Materials

Poly(ethylene terephthalate) (PET) was obtained as a bottle-grade polymer ( $MW=33\,000$ ) in pellet form. Poly(hydroxybutyric acid) (PHBA) ( $MW=670\,000$ ) was obtained from Aldrich in powder form. Poly(*m*-xylylene adipamide) (MXD6) was Mitsubishi grade 6001 (intrinsic viscosity =  $0.65\text{ dl g}^{-1}$ ). Two samples of poly(vinylidene fluoride) (PVDF) were obtained, one from Polysciences Inc. in pellet form ( $MW=100\,000$ ) and one from Aldrich in powder form ( $MW=500\,000$ ). Nylon-6,6 was obtained from ICI in the form of granules (type R6600). Poly(oxymethylene) (POM) was obtained from Aldrich in the form of beads. Lithium trifluoromethanesulfonate (lithium triflate) was obtained from Aldrich. All the above samples were dried in a vacuum oven prior to use.

The solvents (low-molecular-weight compounds) (Table 1) were obtained from various chemical suppliers and dried over molecular sieve before use.

### Gel composition

In these systems it is possible to calculate the lithium-ion concentration relative to the other components in various ways that make different assumptions about the nature of the complex formation. Lithium ions may be regarded as complexing solely with the solvent or alternatively with the polymer and the solvent. In addition the nature of the complex in each case is not clearly identified. Lithium contents in polymer electrolytes are usually expressed in terms of an O/Li ratio based on the atomic concentration of each element, but only those oxygen atoms believed to complex with lithium are

included in the calculation. Thus aliphatic ether and amide oxygen atoms are included, but the oxygen atoms of ester groups are excluded.

In calculating the O/Li ratios for the gel systems investigated in this paper, no account has been taken of the possibility that the lithium may complex with the fluorine atoms of PVDF. In the case of propylene carbonate (PC), only the carbonyl oxygen has been included in the calculation; and in the case of dimethylsulfoxide (DMSO), the ratio is based on the sulfoxide oxygen.

Thus the O/Li ratios quoted in this paper are given by the following formula, where  $n$  is the number of 'active' oxygen atoms per molecule of the solvent, as outlined above:

$$\text{O/Li} = \frac{\text{mass of solvent}}{\text{mass of salt}} \times \frac{MW \text{ of salt}}{MW \text{ of solvent}} \times n \quad (1)$$

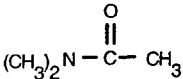
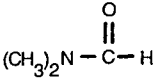
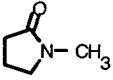
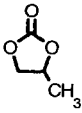
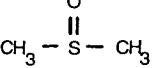
The polymer concentrations quoted are percentage by mass based on the polymer and solvent present, irrespective of the salt content.

As an example of our sample notation: 40/PVDF/DMF refers to a sample of PVDF and dimethylformamide (DMF) in the ratio 40/60 by mass, whereas 40/PVDF/DMF/Li refers to a sample of PVDF, DMF and lithium triflate where the ratio of PVDF to DMF is still 40/60 and the salt content can be calculated from the O/Li ratio using equation (1). All samples have O/Li ratios of 12/1 unless otherwise stated.

### Gel preparation

Gel preparation was undertaken in a glove-box purged with a flow of oxygen-free nitrogen for at least 16 h prior to and during the experimentation. Weighed amounts of polymer, salt and solvent were mixed and heated (with intermittent stirring) until the mixture became homo-

Table 1 Properties of solvents used

Solvent <sup>a</sup>	Structure	Molar mass (g)	M.p. (°C)	B.p. (°C)	Density (g cm <sup>-3</sup> )	Viscosity at 25°C (mPa s)	Dielectric constant
DMA		87.12	-20	164	0.937	1.07	
DMF		73.10	-61	153	0.944	0.80	36.7
NMP		99.13	-24	202	1.026	2.15	32.0
TG	CH <sub>3</sub> (OCH <sub>2</sub> CH <sub>2</sub> ) <sub>4</sub> OCH <sub>3</sub>	222.28	-30	275	1.01	3.54	
PC		102.09	-55	240	1.21	2.35	66.1
DMSO		78.13	18	189	1.101	2.00	46.7

<sup>a</sup> DMA ≡ *N,N*-dimethylacetamide; DMF ≡ *N,N*-dimethylformamide; NMP ≡ *N*-methyl-2-pyrrolidinone; TG ≡ tetraethylene glycol dimethyl ether; PC ≡ propylene carbonate; DMSO ≡ dimethylsulfoxide

geneous. On cooling, a gel was formed. The samples were then reweighed to check whether any solvent loss had occurred, and stored in sealed containers in a desiccator.

### Ionic conductivity

Gel samples were reheated until they flowed and were then cast onto a stainless-steel electrode, which was blocking to both lithium and triflate ions. Initially this operation was carried out in a fume cupboard. In the case of the detailed studies of the PVDF gels, however, all casting was carried out in the glove-box. A second stainless-steel electrode was rapidly brought into contact with the sample so that it was sandwiched between the two electrodes and good contact was achieved with both. A PTFE spacer was used to ensure a constant interfacial separation between the two electrodes. The contact area  $A$  and electrolyte thickness  $t$  were accurately known; in all cases  $A$  was  $1.0\text{ cm}^2$  and  $t$  was in the range 0.3 to 2.0 mm.

The prepared cell was then immediately transferred, in a desiccator, to the chamber in which the conductivity measurements were carried out. This was flooded with dry nitrogen to prevent exposure of the cell to the atmosphere. Brass plates were used to provide electrical contact with both electrodes. Temperature control was achieved by passing the dry nitrogen over a heat exchanger prior to entering the chamber; a thermocouple positioned near the cell was used to monitor the temperature, which was controlled by a Eurotherm temperature control unit. The system was calibrated under experimental conditions to give accurate sample temperatures. A schematic diagram of the apparatus is given in Figure 1.

A Schlumberger 1260 impedance/gain-phase analyser was used to measure the complex admittance of the cell over the frequency range 1 Hz to 400 kHz. Owing to the ion-blocking nature of both electrodes, the real part of the admittance rose to an essentially frequency-independent plateau above around 10 kHz. Initially the bulk gel electrolyte resistance  $R_b$  was determined from this plateau and was used to calculate the ionic conductivity  $\sigma$  from the expression:

$$\sigma = \frac{1}{R_b} \times \frac{t}{A}$$

Latterly it was found that representing the data in the complex impedance plane, and determining  $R_b$  from the intersection of the low-frequency spike with the real impedance axis<sup>15</sup>, gave results that corresponded exactly

with those obtained from the admittance method described above. As a consequence, the ionic conductivity results presented here have been obtained from complex-impedance-plane plots.

The ionic conductivities of gel electrolytes were measured on a single cooling cycle from  $+80$  to  $-20^\circ\text{C}$ . Liquid electrolytes (i.e. without polymer) were contained in a sealed glass tube and a modified Philips PW9550/60 conductivity cell was used to measure the conductivity. The cell employed platinum electrodes and had a fixed cell constant of  $0.82\text{ cm}^{-1}$ . The ionic conductivities of the liquid electrolytes were measured on a single heating cycle, from  $-20$  to  $+80^\circ\text{C}$ .

### Mechanical properties

Gel electrolytes were reheated until they flowed, then cast into discs of diameter 25 mm and thickness approximately 2 mm ( $\pm 0.3$  mm). These discs were placed between parallel circular disc platens of 25 mm diameter in a Rheometrics Dynamic Spectrometer RDS2, at ambient temperature ( $18$  to  $23^\circ\text{C}$ ) in a nitrogen atmosphere, and squeezed under an axial load up to 1 kg. Two mechanical measurements were made, as follows.

**Dynamic modulus  $G'$  and  $G''$ .** One of the disc platens oscillated sinusoidally, at frequencies between 0.016 and 79.6 Hz, about its cylindrical axis of symmetry with constant amplitude. The in-phase component of the measured sinusoidal shear stress was used to determine the dynamic modulus  $G'$  and the out-of-phase component was used to determine the loss modulus  $G''$ .

**Relaxation modulus  $G(t)$ .** Using the same geometry as above, a step shear strain of 1% was applied. The stress then decayed from its maximum as a function of time and the modulus  $G(t)$  is quoted after a relaxation time of 2 min.

### X-ray diffraction

Wide-angle X-ray diffraction analysis was carried out on a Spectrolab Series 3000 diffractometer with Inel XRG-3000 X-ray generator and Inel CPS-120 curved position-sensitive detector. The maximum resolution of the detector allowed data points to be taken at  $0.03^\circ$  intervals. Slit-collimated  $\text{Cu K}_\alpha$  radiation of wavelength 0.1541 nm was generated by voltage and current settings of 40 kV and 16 mA, respectively, and by use of a nickel filter and monochromator.

The gel film was mounted between two brass plates with a hole in the centre to allow the X-ray beam through. The sample and holder were positioned at the centre of curvature of the detector and the diffraction patterns were obtained at room temperature. A microprocessor running Inel software was used to store and analyse the data.

Analysis involved fitting a baseline to the diffraction patterns and curve fitting Gaussian lineshapes to determine peak positions and halfwidths, from which  $d$ -spacings and approximate crystal sizes could be calculated, the latter by use of the Scherrer equation:

$$L_{hkl} = \frac{k\lambda}{\beta \cos \theta} \quad (2)$$

where  $k=0.89$ ,  $\beta$  is the halfwidth and  $L_{hkl}$  is the size normal to the  $hkl$  planes.

All the diffraction patterns possessed a very broad peak ( $\sim 7^\circ$  halfwidth) centred at  $\sim 20^\circ\text{C}$ . This has been

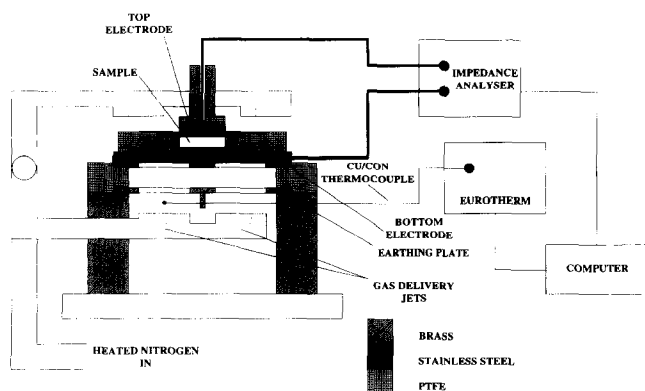


Figure 1 Schematic diagram of the conductivity apparatus

**Table 2** Summary of gel properties. All gels have O/Li=12/1

Sample no.	Polymer	Solvent	Polymer content (%) <sup>a</sup>	Ambient conductivity (S cm <sup>-1</sup> )	Dynamic modulus G' (Pa) <sup>b</sup>	Relaxation modulus G(t) (Pa) <sup>c</sup>	Comment
1	PVDF	DMF	41	6.6 × 10 <sup>-3</sup>	3 × 10 <sup>5</sup>	2 × 10 <sup>5</sup>	Transparent elastic film
2	PVDF	DMSO	38	4.6 × 10 <sup>-3</sup>	2 × 10 <sup>5</sup>	1 × 10 <sup>5</sup>	
3	PVDF	TG	40	2.0 × 10 <sup>-4</sup>	1 × 10 <sup>5</sup>	7 × 10 <sup>4</sup>	
4	PET	NMP	43	2.0 × 10 <sup>-3</sup>	2 × 10 <sup>5</sup>	1 × 10 <sup>5</sup>	Opaque and waxy
5	PHBA	DMA	18	3.6 × 10 <sup>-3</sup>	3 × 10 <sup>5</sup>	— <sup>d</sup>	
6	PHBA	DMA	31	1.5 × 10 <sup>-3</sup>	1 × 10 <sup>5</sup>	7 × 10 <sup>4</sup>	
7	MXD6	NMP	17	2.4 × 10 <sup>-3</sup>	2 × 10 <sup>5</sup>	1 × 10 <sup>5</sup>	
8	Nylon-6,6	NMP	10	2.2 × 10 <sup>-3</sup>	4 × 10 <sup>4</sup>	— <sup>d</sup>	
9	POM	NMP	30	2.9 × 10 <sup>-4</sup>	5 × 10 <sup>4</sup>	3 × 10 <sup>4</sup>	

<sup>a</sup> Polymer content is expressed as a mass percentage of the polymer plus solvent content

<sup>b</sup> G' measured at room temperature for a 1% strain amplitude, at a frequency of 10 Hz

<sup>c</sup> G(t) quoted 2 min after application of 1% strain, at room temperature

<sup>d</sup> Sample not of good enough quality for experiment

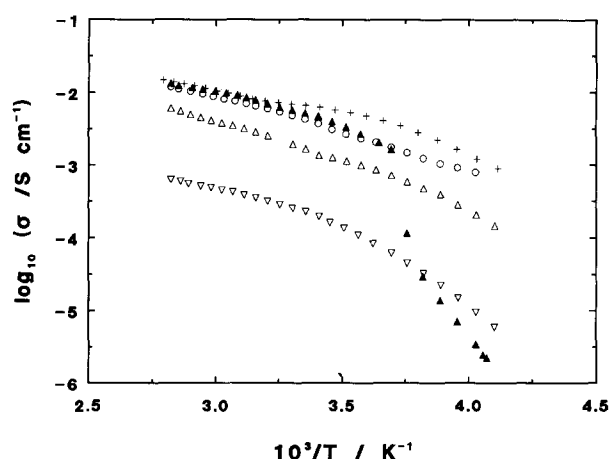


**Figure 2** Arrhenius plot of the conductivity of PVDF gels made with various solvents: (+) DMF; (○) DMA; (▲) DMSO; (△) NMP; (▽) TG. All gels have O/Li=12/1 and polymer content 40%

attributed to scattering from the solvent and amorphous polymer.

#### Thermogravimetric analysis

Thermogravimetric analysis (t.g.a.) was carried out on a DuPont 951 thermogravimetric analyser controlled by DuPont Thermal Analyst 2000 operating software. Samples were heated at 20°C min<sup>-1</sup> to 350°C under a flow of nitrogen. Isothermal analyses were carried out in air by maintaining a constant temperature for 60 min.

## RESULTS AND DISCUSSION

Thermoreversible gels have been made from a variety of polymers and solvents by gel casting from high-temperature solutions. *Table 2* summarizes results for nine such samples. With the exception of samples 3 and 9, room-temperature conductivities are in excess of 10<sup>-3</sup> S cm<sup>-1</sup>, and with the exception of samples 8 and 9, all have storage modulus (G') in excess of 10<sup>5</sup> Pa. The fact that these gels are thermoreversible makes them readily processable.

**Table 3** Room-temperature conductivities of liquid and gel electrolytes

Sample	σ (S cm <sup>-1</sup> )
DMF/Li 100/1	5.4 × 10 <sup>-3</sup>
30/PVDF/DMF/Li (O/Li=100/1)	1.5 × 10 <sup>-3</sup>
40/PVDF/DMF/Li (O/Li=100/1)	1.1 × 10 <sup>-3</sup>
DMF/Li 18/1	1.5 × 10 <sup>-2</sup>
30/PVDF/DMF/Li (O/Li=18/1)	5.6 × 10 <sup>-3</sup>
40/PVDF/DMF/Li (O/Li=18/1)	3.2 × 10 <sup>-3</sup>

The gels made from PVDF, which are transparent, self-supporting and exhibit a good degree of elasticity, were studied in more detail.

#### Ionic conductivity

The variation with temperature of the ionic conductivity σ of PVDF gels prepared from various solvents is shown in the Arrhenius plot of *Figure 2*, which indicates that, at a given polymer concentration and O/Li ratio, the conductivity of the gel is dependent on the nature of the solvent used. Higher conductivities are achieved in the more volatile and less viscous solvents, DMSO being an exception. The conductivity of the gel containing DMSO falls off rapidly at lower temperatures as a consequence of the relatively high (18°C) melting point of the solvent.

A range of DMF–lithium triflate liquid electrolytes have been prepared that have O/Li ratios in the range 100/1 to 18/1. A direct comparison has been made between the ionic conductivities of these liquid electrolytes and gel electrolytes of 30% and 40% PVDF content. *Table 3* shows a comparison of the room-temperature (20°C) conductivities obtained in a selection of the liquid and gel electrolytes. As the salt concentration is increased, the ionic conductivity rises in both the liquids and the gels (at constant PVDF content), although recent evidence suggests that at higher salt concentrations the conductivity reaches a maximum. The addition of increasing amounts of polymer to a liquid electrolyte reduces the conductivity, but the mechanical properties are improved.

The Arrhenius plot in *Figure 3* shows the increase in the ionic conductivity of the liquid electrolytes as the salt

concentration is increased. The curvature of the plots suggests that fitting the data to the Vogel–Tamman–Fulcher (VTF) equation:

$$\sigma(T) = AT^{-1/2} \exp\left(\frac{-B}{T-T_0}\right) \quad (3)$$

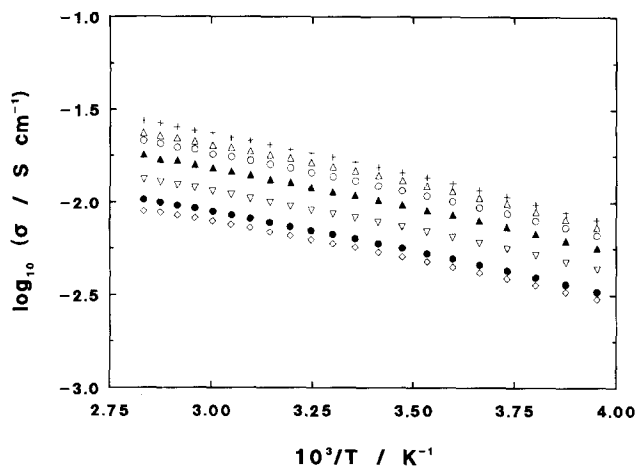


Figure 3 Arrhenius plot of ionic conductivity of liquid electrolytes made from DMF with various salt concentrations: (+) 18/1; (△) 24/1; (○) 30/1; (▲) 40/1; (▽) 60/1; (●) 80/1; (◇) 100/1

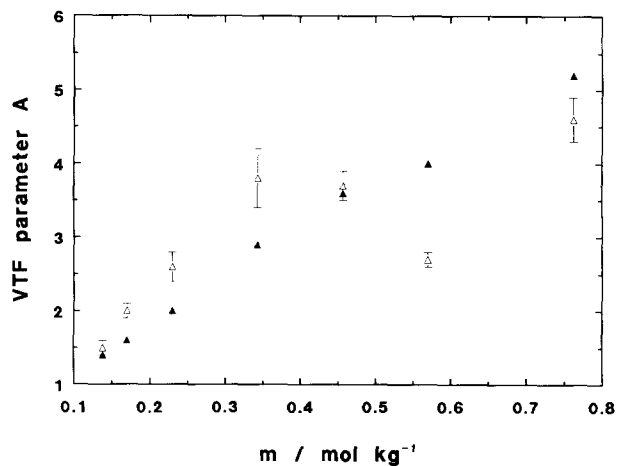


Figure 4 VTF parameter  $A$  from (△) three-parameter fits and (▲) two-parameter fits

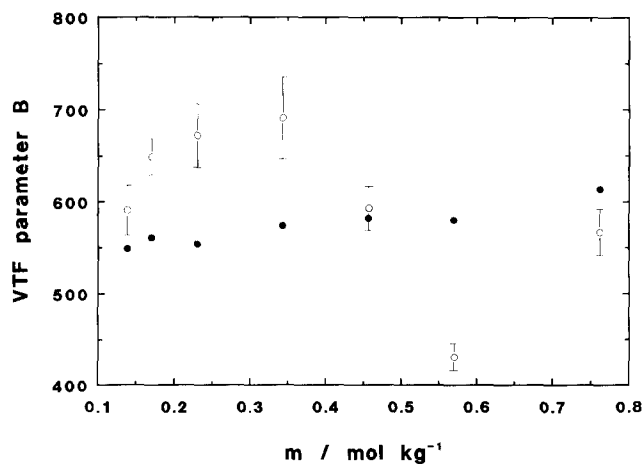


Figure 5 VTF parameter  $B$  from (○) three-parameter fits and (●) two-parameter fits

might be appropriate. Here the pre-exponential factor  $A$  is proportional to the number of charge carriers in the system,  $B$  is akin to an activation energy and  $T_0$  is the equilibrium or 'ideal' glass transition temperature of the system. It is common to assume that  $T_0$  is related to the thermodynamic glass transition  $T_g$  through an expression of the form:

$$T_0 \approx T_g - 50 \text{ K} \quad (4)$$

A FORTRAN routine has been developed that returns the values of  $A$ ,  $B$  and  $T_0$  from three-parameter fits to the conductivity–temperature data. The values of the three parameters, and their variation with salt concentration, are shown in Figures 4, 5 and 6. Here it can be seen that three-parameter fitting, over the fairly narrow temperature range available, does not produce clear trends.

In an attempt to determine sensible trends from the VTF analysis, two-parameter fits have been carried out on the liquid electrolyte data by fixing the value of  $T_0$ . In this case, the mean value of  $T_0$  obtained in the three-parameter fitting ( $84 \pm 7 \text{ K}$ ) has been used for each data set. The values of  $A$  and  $B$  obtained in these new two-parameter fits are also shown in Figures 4 and 5. We now see that  $A$  rises steadily with increasing salt concentration, reflecting the increase in the number of charge carriers, while  $B$  increases slightly over this range of concentration.

While it seems that two-parameter fits offer the chance of deducing trends in the VTF parameters, we must assess the validity of this treatment of  $T_0$ . In many VTF analyses of conductivity data,  $T_0$  is assumed to be related to the glass transition temperature through equation (4).  $T_g$  is found, in general, to increase with increasing salt concentration. In some cases though, for example the liquid polymer electrolytes of Cameron *et al.*<sup>16</sup>,  $T_0$  was found to remain approximately constant at the salt concentrations investigated.

It therefore seems not unreasonable to make the assumption that  $T_0$  remains constant in the liquid electrolytes. We must also ask, however, whether or not the value of  $T_0$  substituted in the two-parameter fits has any physical significance. If we assume that the liquid electrolytes have a glass transition, the temperature of

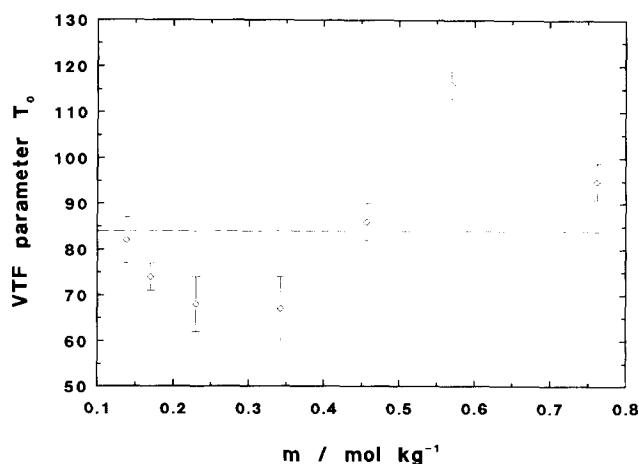


Figure 6 VTF parameter  $T_0$  from (◇) three-parameter fits. The horizontal line represents the average of all the values

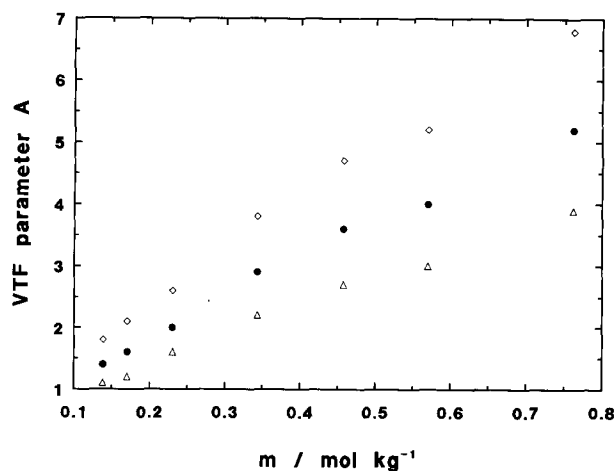


Figure 7 Effect on VTF parameter  $A$  when  $T_0$  is changed by  $\pm 20$  K: (●)  $T_0$ ; ( $\Delta$ )  $T_0 + 20$ ; ( $\diamond$ )  $T_0 - 20$

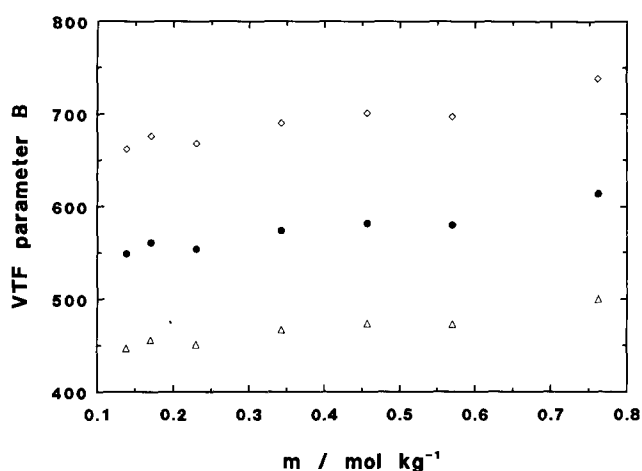


Figure 8 Effect on VTF parameter  $B$  when  $T_0$  is changed by  $\pm 20$  K: (●)  $T_0$ ; ( $\Delta$ )  $T_0 + 20$ ; ( $\diamond$ )  $T_0 - 20$

which is related to the melting point  $T_m$  by the equation<sup>17</sup>:

$$T_g \approx \frac{2}{3}T_m \quad (5)$$

then, using equation (4), we can approximate  $T_0$  as:

$$T_0 \approx \left(\frac{2}{3}T_m\right) - 50 \text{ K} \quad (6)$$

Using the melting point of pure DMF of  $T_m = 212$  K, which it should be noted is depressed by the addition of salt, we generate a value of  $T_0 = 91$  K. This is in good agreement with the value of  $T_0 = 84 \pm 7$  K used in the two-parameter fits. Indeed, the value of  $T_0$  can be altered by  $\pm 20$  K without affecting the trends observed in either  $A$  or  $B$ , as shown in Figures 7 and 8. It therefore seems that, in this qualitative form of analysis, the exact choice of the value of  $T_0$  is not particularly crucial.

In order to examine how changes in the conductivity of the liquid electrolytes scale with salt concentration, the molal conductivity  $\Lambda_m$  is plotted in Figure 9. Molal conductivity is defined by the expression:

$$\Lambda_m = \sigma/m \quad (7)$$

Figure 9 shows that, as the electrolytes become more concentrated, the molal conductivity falls. If it is assumed that these systems can be classified as strong electrolytes, then the fall in molal conductivity can be attributed to increasing interaction between the solvated ions. Of

particular interest is whether this fall is due to the existence of ionic association. This is being investigated through further conductivity studies, pulsed field gradient spin-echo n.m.r. and Raman spectroscopy techniques.

Table 3 has shown clearly that, as expected, the formation of a gel reduces the conductivity of the liquid electrolyte from which it is prepared. It is important to determine exactly how this arises—whether the presence of the gel network reduces conductivity through simple geometrical effects, or whether there is some kind of specific interaction between the polymer and the salt.

Figure 10 plots the variation in conductivity with salt concentration of the liquid electrolytes and the 30% PVDF gels in which they are incorporated. It can be seen that there appears to be a constant scaling factor between a given liquid and gel, with the ratio of gel conductivity to liquid conductivity being around 0.35 at all salt concentrations. The 40% PVDF gels have been prepared at O/Li = 100/1 and 18/1, and again there is a constant gel/liquid conductivity ratio of 0.21. These observations suggest that the liquid electrolyte can be thought of as being essentially decoupled from the supporting gel network.

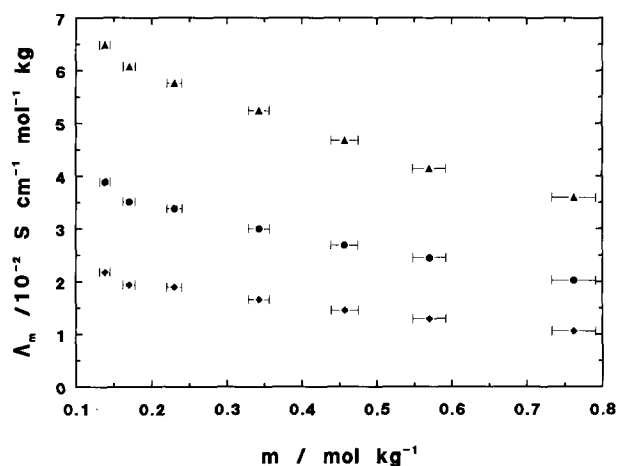


Figure 9 Variation of molal conductivity with salt concentration at various temperatures: ( $\blacktriangle$ ) 80°C; ( $\bullet$ ) 20°C; ( $\blacklozenge$ ) -20°C

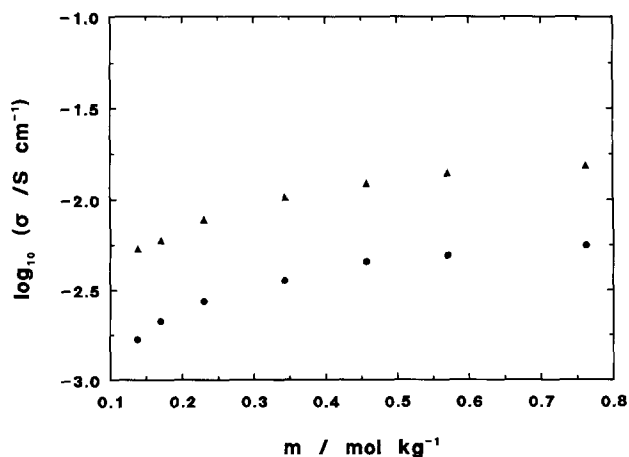


Figure 10 Conductivity as a function of salt concentration for ( $\blacktriangle$ ) DMF liquid electrolyte and ( $\bullet$ ) 30% PVDF gel made from the liquid electrolyte

## Compositional stability

Although it is envisaged that these conducting gels will be used in enclosed systems, we have studied the loss of solvent in an unenclosed system. Figure 11 shows the mass percentage of PVDF/TG gel remaining when heated at  $20^{\circ}\text{C min}^{-1}$  to  $350^{\circ}\text{C}$ . Analysis of Figure 11 reveals that increasing the polymer concentration of unsalted gels from 12% to 39% has a negligible effect on the temperature at which a given percentage of solvent is lost (Figure 12) except at high percentage solvent loss when the gel with higher polymer content offers more resistance to solvent loss. However, incorporating lithium triflate into the gel raises the temperature at which a given percentage of solvent is lost (Figure 13). This increase in temperature is greater the higher the polymer concen-

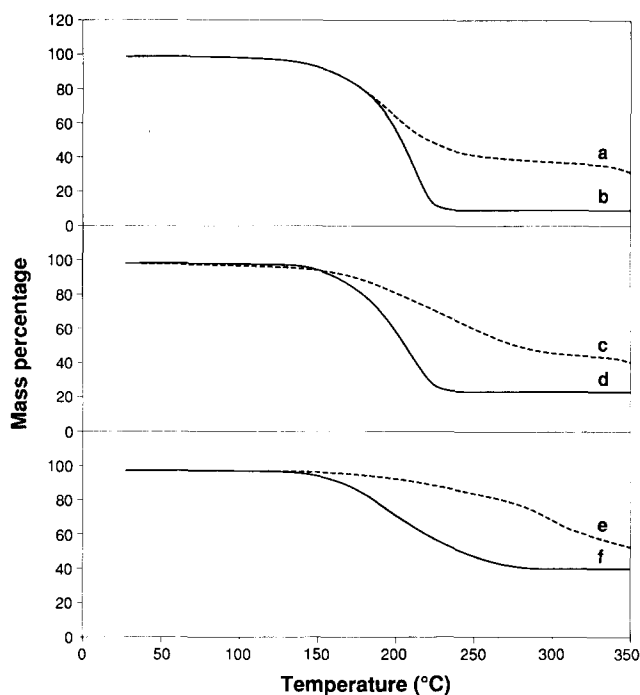


Figure 11 Percentage mass of PVDF/TG gels remaining as heated at  $20^{\circ}\text{C min}^{-1}$ : (a) 12/PVDF/TG/Li; (b) 12/PVDF/TG; (c) 25/PVDF/TG/Li; (d) 25/PVDF/TG; (e) 39/PVDF/TG/Li; (f) 39/PVDF/TG

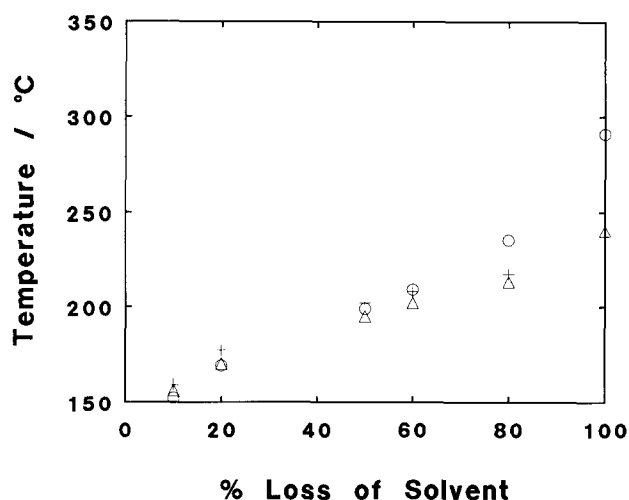


Figure 12 Temperature at which a given percentage of solvent is lost from unsalted PVDF/TG gels: (+) 12% polymer; ( $\Delta$ ) 25% polymer; ( $\circ$ ) 39% polymer

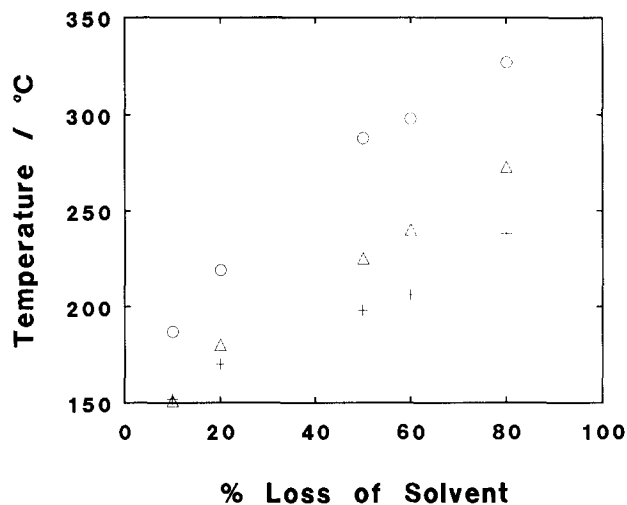


Figure 13 Temperature at which a given percentage of solvent is lost from salted PVDF/TG gels with O/Li = 12/1: (+) 12% polymer; ( $\Delta$ ) 25% polymer; ( $\circ$ ) 39% polymer

Table 4 Percentage loss of solvent from salted and unsalted 25/PVDF/TG gels when maintained at constant temperature for an hour

Temperature ( $^{\circ}\text{C}$ )	Loss of solvent in one hour (%)	
	25/PVDF/TG	25/PVDF/TG/Li
75	5.3	
96	10.5	
115	44.7	32.9

tration, and is particularly noticeable at high percentage solvent loss. For example, the temperatures at which 80% of the solvent is lost from unsalted and salted 12/PVDF/TG are 217 and  $238^{\circ}\text{C}$  respectively, whereas for 39/PVDF/TG the temperatures are 235 and  $327^{\circ}\text{C}$  respectively.

The increase in stability due to addition of salt is attributed to complexation between the salt and solvent, making the solvent less volatile. The improved stability due to increase in polymer content is attributed to the more tortuous path that the solvent molecules have to take to escape.

Isothermal t.g.a. for 1 h revealed the mass loss of 25/PVDF/TG gels to be linear with time. Table 4 shows that incorporating salt reduces the rate of loss of the solvent. This increased stability due to the presence of salt is attributed to complexation, reducing the volatility of the solvent.

The percentage mass loss of solvent after 1 h at a given temperature is highly dependent on the nature of the solvent. For example, at a constant temperature of only  $66^{\circ}\text{C}$ , all the solvent was lost from 40/PVDF/DMF/Li (O/Li = 18/1) within 30 min.

## Crystalline structure

The gels reported are all thermoreversible in nature and thus it is believed that many of the junction zones are of a physical nature. WAXD has been employed to determine the crystalline structure of the gels. Figure 14 shows diffraction patterns for unsalted and salted gels of 39/PVDF/TG and 43/PVDF/DMF. It is immediately noticeable that the presence of salt has a marked effect

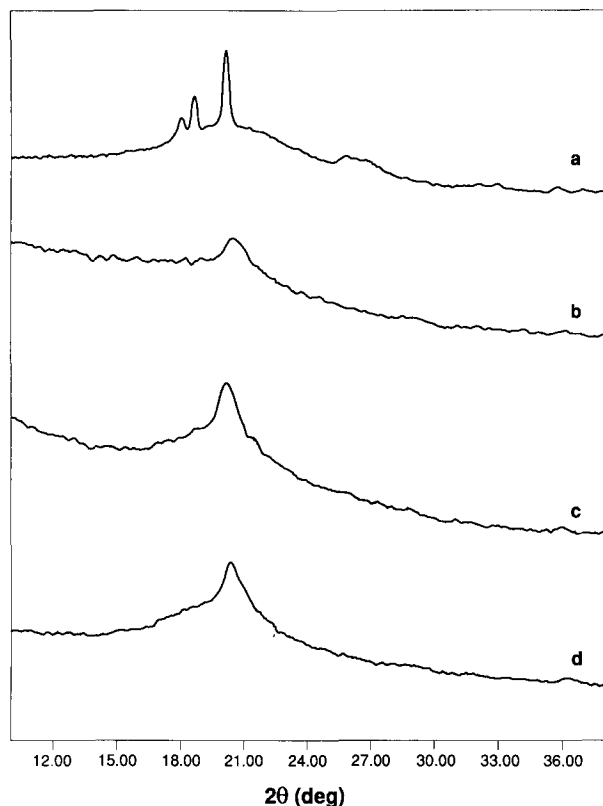


**Figure 14** X-ray diffraction patterns of salted and unsalted gels: (a) 39/PVDF/TG; (b) 39/PVDF/TG/Li; (c) 43/PVDF/DMF; (d) 43/PVDF/DMF/Li

on the structure of gels made with TG, whereas it appears to have no effect on the structure of gels made with DMF.

PVDF crystallizes with five different structures<sup>18–20</sup>. From the existence of the peak at 17.9° in the diffraction pattern of *Figure 14a* it appears that the unsalted gels of 39/PVDF/TG crystallize in the  $\alpha$  phase. This is in agreement with Doll and Lando<sup>21</sup>, who found that PVDF crystallizes in the  $\alpha$  phase from non-polar solvents, TG being a non-polar solvent.

A reason for the difference in structure between the unsalted and salted 39/PVDF/TG gels may be direct complexing of the salt with the polymer. This idea is supported by the work of Grubb *et al.*<sup>22</sup>, who found that in the presence of ionic impurities PVDF is more likely to crystallize in the  $\gamma$  phase. They suggest that this is due to the ions being attracted to the polar faces of the  $\gamma$  unit cell, thus reducing the electrostatic energy of the system. This would thus promote the growth of the polar  $\gamma$  phase in a system where there is a delicate balance between polar and non-polar growth.

It is difficult to determine the phase exhibited in

diffraction pattern *Figure 14b* since the peak at  $\sim 20^\circ$  is present for all PVDF phases. The  $\gamma$  phase can be identified by the presence of a weak 111 reflection at  $\sim 22.5^\circ$ , but it is difficult to say if this peak is present or not in *Figure 14b*. The absence of a peak at 17.9° suggests that we have the  $\gamma$  or  $\beta$  phase, and in view of the work by Grubb *et al.* we shall assume we have the  $\gamma$  phase.

DMF, a highly polar solvent, does not cause this difference in crystal structure when salt is added to the gel. This is probably because the unsalted gel is already crystallized in the  $\gamma$  phase; Gal'Perin *et al.*<sup>23</sup> report that the  $\gamma$  phase is formed when PVDF is crystallized from DMF.

Salted gels have been made with other solvents (DMA, DMSO, NMP and PC) and their diffraction patterns are very similar to *Figures 14b* and *14d*, i.e. to those of the salted gels made from TG and DMF.

*Table 5* shows the crystal sizes determined from equation (2) for the dominant peaks in the diffraction patterns shown in *Figure 14*. Although the proportions of crystalline material appear to be low, the diffraction peaks of 39/PVDF/TG are sharp, indicating a small number of crystalline regions of reasonable size. For the diffraction patterns of *Figures 14b–d* the crystal sizes quoted are a lower limit, since the dominant peaks may in fact consist of two peaks superimposed.

WAXD of a 25/PET/NMP/Li gel showed the presence of weak peaks characteristic of PET, thus showing that at least some of the polymer is in a crystalline form.

#### Mechanical properties

As already stated, the PVDF gels could be cast into tough and readily handleable films. To quantify the mechanical properties of these films, the gels were subjected to oscillatory shear as described above. The storage modulus ( $G'$ ) and the loss modulus ( $G''$ ) remained approximately constant over the frequency range covered, but they showed a marked decrease with increasing strain amplitude (*Figure 15* and *Table 2*). At low strain amplitude ( $\sim 1\%$ )  $G'$  (approximately  $10^5$  Pa) dominates  $G''$  and the samples can be described as elastic (*Figure 16*). At high strain amplitude ( $\sim 20\%$ ) it is  $G''$  that dominates  $G'$ . It thus appears that at high strains the gel network is breaking down in some way, although this breakdown is completely recoverable when the strain is removed. A typical graph of relaxation modulus  $G(t)$  is shown in *Figure 17*, and it is seen that 2 min after the strain was applied this modulus has reached an approximately constant value.

Good contact between the sample and the platens was sometimes difficult to achieve and increased axial load had to be applied. In some cases this slightly increases the modulus (an effect attributed to loss of solvent).

**Table 5** Crystal sizes calculated from peak widths

Approx. $2\theta$ (deg)	Crystal size (nm)			
	39/PVDF/TG	39/PVDF/TG/Li	43/PVDF/DMF	43/PVDF/DMF/Li
18	25			
19	40			
20	31	6	8	10
26	13			
27	3			
36			9	7



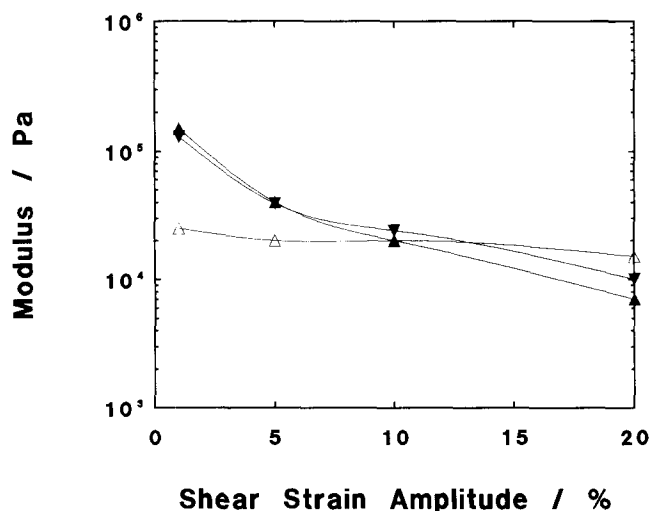


Figure 15 Room-temperature variation of moduli with strain amplitude for 38/PVDF/DMSO/Li gel recorded at 0.016 Hz: ( $\blacktriangle$ )  $G'$ ; ( $\triangle$ )  $G''$ ; ( $\blacktriangledown$ )  $G(t)$

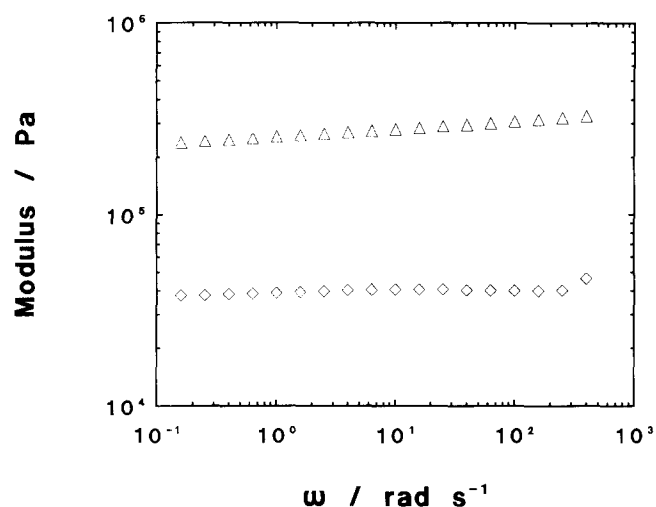


Figure 16 Room-temperature variation of moduli with frequency for 41/PVDF/DMF/Li for a 1% strain amplitude: ( $\triangle$ )  $G'$ ; ( $\diamond$ )  $G''$

The PET/NMP gels possessed similar mechanical properties to those of the PVDF gels, i.e.  $G'$  and  $G''$  were linear in the frequency range covered, and  $G'$  and  $G(t)$  were highly strain-dependent, with  $G'$  dominating  $G''$  at low strain. Thus at low strain these materials can be described as gels according to the definition of Almdal<sup>14</sup> above.

## CONCLUSIONS

Thermoreversible conducting gels have been prepared from various polymers and high-temperature solvents by gel casting, incorporating lithium trifluoromethanesulfonate as the ionic species necessary for conduction. The majority of these gels have ionic conductivities about  $10^{-3} \text{ Scm}^{-1}$  (the generally accepted lower limit for commercial exploitation) even at temperatures of  $-20^\circ\text{C}$ . Other factors to be considered for a commercial product are the mechanical rigidity of the gel and the volatility of the solvent. We have shown that increasing the polymer content of the gel increases the stiffness but reduces ionic conductivity. Increasing the salt concentration increases conductivity and reduces the volatility of the solvent. A compromise in the gel composition is

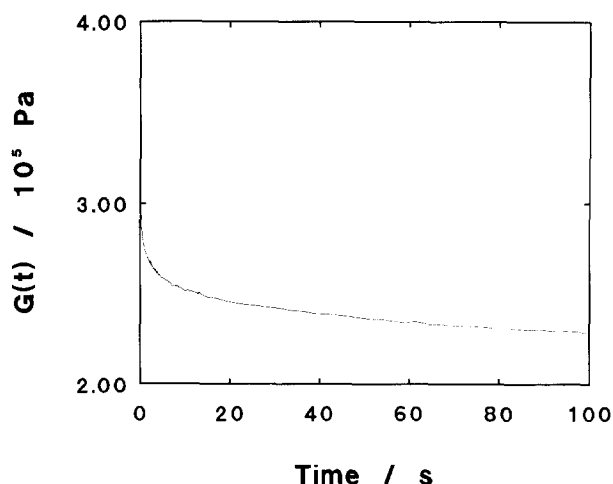


Figure 17 Room-temperature stress relaxation modulus of 41/PVDF/DMF/Li gel for a 1% step shear strain

thus needed to obtain a material with high ionic conductivity and yet maintaining good mechanical and thermal properties.

Such gels contain a higher proportion of ion-complexing solvent than is available in plasticized compositions, do not require an ion-complexing polymer and are advantageously made using crystallizable polymers. Of all the polymers used in this investigation, gels made from PVDF were the best, since they had satisfactory mechanical properties at low strain, high ambient ionic conductivity and were optically transparent.

Both PVDF and PET gels were shown to have a modulus that decreased rapidly with strain, but which was approximately independent of strain rate in the frequency range considered. This loss of elastic response with strain, which was attributed to breakdown of the gel network, was completely recoverable.

The presence of salt has a large effect on the properties of these gels. The crystal phase of PVDF in TG was changed from  $\alpha$  to  $\gamma$  by the addition of salt. Solvent evaporation rates decreased with the addition of salt. Ionic conductivity increased with increasing salt concentration, although it has been shown that at these high concentrations there may be a considerable degree of ionic association.

Whether the salt has any interaction with the polymer is still to be established. Ionic conductivity experiments on liquid electrolytes and derived gels suggest that there is no interaction between salt and polymer. On the other hand, the fact that the salt so greatly affects the crystallization of PVDF in TG suggests the possible presence of such an interaction in this case.

## REFERENCES

- 1 Fenton, B. E., Parker, J. M. and Wright, P. V. *Polymer* 1974, **14**, 58
- 2 Armand, M. B. in 'Fast Ion Transport in Solids' (Eds, P. Vashishta *et al.*), Elsevier North-Holland, Amsterdam, 1979
- 3 Bannister, D. J., Davies, G. R., Ward, I. M. and McIntyre, J. E. *Polymer* 1984, **25**, 1600
- 4 Dobrowski, S. A., Davies, G. R., McIntyre, J. E. and Ward, I. M. *Polymer* 1991, **32**, 2887
- 5 Ballard, D. G. H., Cheshire, P., Mann, T. S. and Przeworski, J. E. *Macromolecules* 1990, **23**, 1256
- 6 Tsuchida, E., Ohno, H. and Tsunemi, K. *Electrochim. Acta* 1983, **28**, 591
- 7 Tsunemi, K., Ohno, H. and Tsuchida, E. *Electrochim. Acta* 1983, **28**, 833

- 8 Matsuda, H., Hiroyuki, O., Mizoguchi, K. and Tsuchida, E. *Polym. Bull.* 1982, **7**, 271
- 9 Watanabe, M., Kanba, M., Matsuda, H., Tsunemi, K., Mizoguchi, K., Tsuchida, E. and Shinohara, I. *Makromol. Chem., Rapid Commun.* 1981, **2**, 741
- 10 Watanabe, M., Kanba, M., Nagoka, K. and Shinohara, I. *J. Polym. Sci., Polym. Phys. Edn.* 1983, **21**, 939
- 11 Kabata, T., Fujii, T., Kimura, O., Ohsawa, T., Matsuda, Y. and Watanabe, M. *Polym. Adv. Tech.* 1993, **4**, 205
- 12 Reich, S. and Michaeli, I. *J. Polym. Sci., Polym. Phys. Edn.* 1975, **13**, 9
- 13 McIntyre, J. E., Ward, I. M., Hubbard, H. V. St A. and Rogers, V., UK Pat. Appl. GB 2260137 A (Apr. 1993)
- 14 Almdal, K., Dyre, J., Hvidt, S. and Kramer, O. *Polym. Gels Networks* 1993, **1**, 5
- 15 Bruce, P. G. in 'Polymer Electrolyte Reviews 1' (Eds. J. R. MacCallum and C. A. Vincent), Elsevier Applied Science, London, 1987
- 16 Cameron, G. G., Ingram, M. D. and Sorrie, G. A. *J. Chem. Soc., Faraday Trans. 1* 1987, **83**(11), 3345
- 17 Kauzmann, W. *Chem. Rev.* 1948, **43**, 219
- 18 Hasegawa, R., Takahashi, Y., Chatani, Y. and Tadokoro, H. *Polym. J.* 1972, **3**, 600
- 19 Bachmann, M., Gordon, W. L., Weinhold, S. and Lando, J. B. *J. Appl. Phys.* 1980, **51**, 5095
- 20 Lovinger, A. J. *Macromolecules* 1981, **14**, 322
- 21 Doll, W. W. and Lando, J. B. *J. Appl. Polym. Sci.* 1970, **14**, 1767
- 22 Grubb, D. T., Cebe, P. and Choi, K. W. *Ferroelectrics* 1984, **57**, 121
- 23 Gal'Perin, Ye. L., Kosmynin, B. P. and Bychkov, R. A. *Vysokomol. Soyedin (B)* 1970, **12**, 555